SIAM J. NUMER. ANAL.
Vol. 42, No. 6, pp. 2298–2319

HIGHER-ORDER FOURIER APPROXIMATION IN SCATTERING BY TWO-DIMENSIONAL, INHOMOGENEOUS MEDIA*

OSCAR P. BRUNO† AND E. MCKAY HYDE‡

Abstract. This paper provides a theoretical analysis of a higher-order, FFT-based integral equation method introduced recently [*IEEE Trans. Antennas and Propagation*, 48 (2000), pp. 1862–1864] for the evaluation of transverse electric–polarized electromagnetic scattering from a bounded, penetrable inhomogeneity in two-dimensional space. Roughly speaking, this method is based on Fourier smoothing of the integral operator and the refractive index $n(x)$. Here we *prove* that the solution of the resulting integral equation approximates the solution of the exact integral equation with higher-order accuracy, *even when* $n(x)$ *is a discontinuous function*—as suggested by the numerical experiments contained in the paper mentioned above. In detail, we relate the convergence rates of the computed interior and exterior fields to the regularity of the scatterer, and we demonstrate, with a few numerical examples, that the predicted convergence rates are achieved in practice.

Key words. Helmholtz equation, Lippmann–Schwinger integral equation, transverse electric scattering, TM scattering, fast Fourier transform

AMS subject classifications. 35J05, 65N12, 65R20, 78A45

DOI. 10.1137/S0036142903425811

1. Introduction.

Scattering problems find application in a wide range of fields, including communications, materials science, plasma physics, biology, medicine, radar, and remote sensing. The evaluation of useful numerical solutions for scattering problems remains a highly challenging problem, requiring novel mathematical approaches and powerful computational tools. An integral equation method [7, 8] introduced recently for the evaluation of time-harmonic, transverse electric (TE)–polarized, electromagnetic scattering by bounded inhomogeneities in two dimensions has proven highly competitive with currently available approaches. (Note that there is some ambiguity in the naming of the polarization [28, p. R5], with some authors referring to this setting as transverse magnetic (TM)–polarized scattering. To be precise, we consider the case in which the electric field is parallel to the cylindrical axis of the scatterer.) In this paper, we provide a theoretical analysis of the higher-order convergence of this approach. More specifically, we *prove* that the approximating integral equation used in this method, which is based on Fourier approximation of the integral

*Received by the editors April 7, 2003; accepted for publication (in revised form) March 25, 2004; published electronically March 31, 2005. This effort was sponsored in part by the Air Force Office of Scientific Research (AFOSR), Air Force Materials Command, USAF, under the AASERT award F49620-98-1-0368. The U.S. Government is authorized to reproduce and distribute reprints for governmental purposes notwithstanding any copyright notation thereon. The views and conclusions contained herein are those of the authors and should not be interpreted as necessarily representing the official policies or endorsements, either expressed or implied, of the Air Force Office of Scientific Research or the U.S. Government.

http://www.siam.org/journals/sinum/42-6/42581.html

†Applied and Computational Mathematics, California Institute of Technology, Pasadena, CA 91125 (bruno@acm.caltech.edu). The research of this author was supported by AFOSR grants F49620-96-1-0008, F49620-99-1-0010, and F49620-02-1-0049; the NSF through the NYI award DMS-9596152 and through contracts DMS-9523292, DMS-9816802, and DMS-0104531; and the Powell Research Foundation.

‡Computational and Applied Mathematics - MS 134, Rice University, 6100 Main St., Houston, TX 77005-1892 (hyde@caam.rice.edu). The research of this author was supported by a DOE Computational Science Graduate Fellowship, an Achievement Rewards for College Scientists (ARCS) Fellowship, and an NSF Mathematical Sciences Postdoctoral Research Fellowship.

operator, yields higher-order convergence in the L^∞-norm even when the refractive index $n(x)$ is a discontinuous function. Furthermore, we relate the convergence rates of the computed interior and exterior fields to the regularity of the scatterer, and we demonstrate, with a few numerical examples, that the predicted convergence rates are achieved in practice.

Given an incident field u^i, we denote by u the total electric field—which equals the sum of u^i and the resulting scattered field u^s:

$$u = u^i + u^s. \tag{1.1}$$

Calling λ the wavelength of the incident field and $\kappa = \frac{2\pi}{\lambda}$ the wavenumber, the total field u satisfies [9, p. 2]

$$\Delta u + \kappa^2 n^2(x) u = 0, \quad x \in \mathbb{R}^3, \tag{1.2}$$

where the given incident field u^i is assumed to satisfy

$$\Delta u^i + \kappa^2 u^i = 0, \quad x \in \mathbb{R}^3. \tag{1.3}$$

Finally, to guarantee that the scattered wave is outgoing, u^s is required to satisfy the Sommerfeld radiation condition [9, p. 67]

$$\lim_{r\to\infty} \sqrt{r}\left(\frac{\partial u^s}{\partial r} - i\kappa u^s\right) = 0. \tag{1.4}$$

The algorithms available for computing solutions to this problem fall into two broad classes: (1) finite element and finite difference methods and (2) integral equation methods. Use of finite element and finite difference methods can be advantageous in that, unlike other methods, they lead to sparse linear systems. Their primary disadvantage, on the other hand, lies in the fact that in order to satisfy the Sommerfeld radiation condition (1.4), a relatively large computational domain containing the scatterer must be used, together with appropriate absorbing boundary conditions on the boundary of the computational domain (see, for example, [10, 17, 18, 26, 32]). Thus, these procedures give rise to very large numbers of unknowns and, thus, to very large linear systems.

A second class of algorithms is based on the use of integral equations. An appropriate integral formulation for our two-dimensional TE problem is given by the Lippmann–Schwinger integral equation [9, p. 214], [24],

$$u(x) = u^i(x) - \kappa^2 \int g(x-y) m(y) u(y) dy, \tag{1.5}$$

where $g(x) = \frac{i}{4} H_0^1(\kappa|x|)$ is the fundamental solution of the Helmholtz equation in two dimensions and m is the *compactly supported* function $m = 1 - n^2$. Integral equation approaches are advantageous in a number of ways: they require only discretization of the equation *on the scatterer itself*, and the solutions they produce satisfy the radiation condition at infinity *automatically*. Direct use of integral equation methods is costly, however, since they lead to dense linear systems: a straightforward computation of the required convolution requires $\mathcal{O}(N^2)$ operations per iteration of an iterative linear solver. As mentioned above, however, the *higher-order* integral method that we analyze in this paper, in which the complexity of the convolution evaluation

is reduced to $\mathcal{O}(N \log N)$ operations per iteration, is highly competitive with finite element or finite difference approaches.

Fast solvers for (1.5), based on the fast Fourier transform (FFT), have been available for some time [3, 31, 33]. In these solvers, the convolution with the fundamental solution is computed via Fourier transforms, which can, in turn, be evaluated with low complexity by means of FFTs. These methods do give rise to a reduced complexity for a given discretization but, unfortunately, they are only first-order accurate for discontinuous scatterers. Low-order accuracy results since, for a general nonsmooth and/or nonperiodic function, the FFT provides a poor approximation to the Fourier transform. Our approach also uses FFTs to achieve a reduced complexity but, unlike previous FFT methods, it yields, in addition, *higher-order accuracy*.

Despite the significant advantages exhibited by higher-order methods over their low-order counterparts (see, for example, Appendix B), only limited attempts have been made to develop higher-order methods for the problem under consideration. A higher-order method was proposed in [23] on the basis of a locally corrected Nyström discretization; the complexity of this method, however, is $\mathcal{O}(N^2)$, where N is the total number of unknowns used.

In [27], Vainikko presents two $\mathcal{O}(N \log N)$ methods for solving (1.5). The first applies to m in the Sobolev space $W^{\mu,2}$ and yields $\mathcal{O}(h^\mu)$ L^2-convergence in the near and the far fields. We instead consider piecewise-smooth $m \in C^{k,\alpha}$ (which are arguably the appropriate spaces for scatterers arising in practice). (For the precise definition of the function spaces that we consider, see Definitions 2.4 and 2.5.) In comparing Vainikko's approach with our method, note that a piecewise-smooth $m \in C^{0,\alpha}$ which does not belong to C^1 can, at best, belong to $W^{2,2}$ [22, p. 197], [11, p. 194], for which Vainikko's method predicts $\mathcal{O}(h^2)$ L^∞-convergence in both the near and the far field. Our method, on the other hand, achieves $\mathcal{O}(h^3)$ and $\mathcal{O}(h^5)$ L^∞-convergence in the near and far fields, respectively (see section 3.2 for our convergence results). More generally, a piecewise-smooth $m \in C^{k,\alpha}$ for $k \geq 1$ which does not belong to C^{k+1} can, at best, belong to $W^{k+2,2}$, for which Vainikko's result predicts $\mathcal{O}(h^{k+2})$ L^∞-convergence in both the near and far field, whereas our method achieves $\mathcal{O}(h^{k+3})$ L^∞-convergence in the near field and $\mathcal{O}(h^{k+6})$ L^∞-convergence in the far field.

The second method proposed in [27] applies to piecewise-smooth (possibly discontinuous) m and yields $\mathcal{O}(h^2(1+|\log h|))$ L^∞-convergence in the near and far fields. (This method requires evaluation of the volume fraction of each discretization cell on each side of a discontinuity in $m = 1 - n^2$.) For such inhomogeneities, our method yields $\mathcal{O}(h^2)$ and $\mathcal{O}(h^3)$ L^∞-convergence in the near and far fields, respectively. Thus, our approach, which applies to smooth as well as discontinuous refractive indices, is both fast—it runs in $\mathcal{O}(N \log N)$ operations—and higher-order accurate, substantially exceeding the convergence rates of Vainikko's approach, especially in the far field.

Our method is based on recasting the last term of the integral equation (1.5) by means of the polar coordinate form

$$(Ku)(a,\phi) = -\kappa^2 \int g(a,\phi;r,\theta) m(r,\theta) u(r,\theta) r \, dr \, d\theta. \tag{1.6}$$

An approximate integral equation is obtained from (1.6) by replacing the kernel g by a truncation of its Fourier representation with respect to its angular variables—which, as is known, is given by the addition theorem for the Hankel function; see section 2. As we show in this paper, the solution of this approximate integral equation approximates the solution of the exact integral equation with higher-order accuracy, even for discontinuous functions $n(x)$.

The higher-order convergence of this method relies on the following important fact: although the Fourier representation of the fundamental solution converges slowly, the resulting Fourier representation of the integral converges *rapidly*; clearly, such accuracy improvements for integrated quantities can only occur through a process of error cancellation. In this paper, we prove that this approach does indeed yield higher-order convergence (at least third-order in the exterior field) even in the case of discontinuous inhomogeneities. More precisely, we derive bounds on the convergence rates for the interior and exterior fields as they depend on the regularity of the scatterer (see Theorem 3.5 and Corollaries 3.9 and 3.10).

Our present analysis considers neither a specific numerical discretization for the radial integration nor the method used to solve the resulting linear system. Here we focus instead on the exact solution of the approximate integral equation resulting from the polar Fourier approximation of the fundamental solution, as described briefly above and in detail in section 2; this exact solution of the approximate equation is to be viewed as an approximate solution of the exact equation (1.5). The details of the complete numerical implementation are given in their original form in [7, 8] as well as in the more recent presentations [5, 14], which contain several significant improvements.

As discussed in section 4, our approximate integral formulation allows us to replace the (possibly discontinuous) function n in polar coordinates by its truncated Fourier series of certain orders *without introducing additional errors*. This fact allows us to compute the corresponding angular integrals *exactly* by means of FFTs. (In [14, 15, 16], similar ideas are used in the construction of a fast, higher-order method for the Helmholtz equation in three dimensions.) To conclude this paper we present a number of computational examples that demonstrate that the predicted convergence rates are achieved in practice.

(Note that a direct application of the methods presented in this paper to discontinuous scatterers for either TM or three-dimensional electromagnetic scattering would yield rates of convergence lower than those for the TE case considered here—since in such cases the normal derivatives of the solution are not continuous across surfaces of discontinuity of the refractive index. As shown in [6], however, the convergence rates of our method for all of these problems—TE, TM, and three-dimensional electromagnetic scattering—can be improved significantly by appropriate treatment of thin volumetric regions around surfaces where either discontinuities or reduced regularity of the refractive index occur.)

2. An approximate integral equation. As mentioned in the introduction, our approach produces numerical solutions of (1.5) through consideration of a sequence of approximate integral equations, which result as the fundamental solution is replaced by a truncated Fourier series in an angular variable. In this section we describe our approximate integral equations, and we show that (1) they admit unique solutions and (2) the inverse operators for the approximate problems are uniformly bounded.

To introduce our approximate integral equations we begin by recalling an addition theorem: using polar coordinates $x = ae^{i\phi}$ and $y = re^{i\theta}$, the addition theorem for the Hankel function reads [9, p. 67]

$$H_0^1(\kappa|ae^{i\phi} - re^{i\theta}|) = \sum_{\ell=-\infty}^{\infty} \mathcal{J}_\ell(a, r)e^{i\ell(\phi-\theta)},$$

where, calling J_ℓ and H^1_ℓ the Bessel and Hankel functions of order ℓ, we have denoted

$$\mathcal{J}_\ell(a,r) = H^1_\ell(\kappa \max(a,r))\ J_\ell(\kappa \min(a,r)). \tag{2.1}$$

This identity allows us to obtain another expression for the integral operator K of (1.5),

$$(Ku)(a,\phi) = -\frac{i\kappa^2}{4}\int H^1_0(\kappa|x-y|)m(y)u(y)dy = \sum_{\ell=-\infty}^{\infty}(K_\ell u)(a)e^{i\ell\phi},$$

where, using an annular region $R_0 \le a \le R_1$ containing the support of m, we have set

$$(K_\ell u)(a) = -\frac{i\kappa^2}{4}\int_{R_0}^{R_1}\mathcal{J}_\ell(a,r)\left[\int_0^{2\pi} m(r,\theta)u(r,\theta)e^{-i\ell\theta}d\theta\right] r\,dr. \tag{2.2}$$

Truncating this Fourier series as well as the corresponding Fourier series for the incident field, we obtain the approximate integral equation

$$v(a,\phi) = u^{i,M}(a,\phi) + (K^M v)(a,\phi), \tag{2.3}$$

where

$$u^{i,M}(a,\phi) = \sum_{\ell=-M}^{M} u^i_\ell(a)e^{i\ell\phi}, \tag{2.4}$$

$$(K^M v)(a,\phi) = \sum_{\ell=-M}^{M}(K_\ell v)(a)e^{i\ell\phi}. \tag{2.5}$$

Here and throughout this paper we use a superscript M to denote the truncated Fourier series of order M of a given function.

Decomposing (2.3) into Fourier modes, we observe that a solution of this equation must satisfy

$$v_\ell(a) = \begin{cases} u^i_\ell(a) + (K_\ell v)(a) & \text{for } |\ell| \le M, \\ 0 & \text{for } |\ell| > M. \end{cases} \tag{2.6}$$

Hence,

$$v(a,\phi) = v^M(a,\phi)$$

and solving (2.3) is equivalent to solving the following system of one-dimensional integral equations:

$$v_\ell(a) - (K_\ell v^M)(a) = u^i_\ell(a), \quad \ell = -M,\dots,M. \tag{2.7}$$

To prove existence and uniqueness for this approximate integral equation, we make use of the following technical lemma.

LEMMA 2.1. *There exists a constant $C > 0$ depending only on R_0, R_1, and κ such that*

$$\left\| \int_{R_0}^{R_1} |\mathcal{J}_\ell(a,r)| r\,dr \right\|_\infty \le \frac{C}{\ell^2},$$

where $\mathcal{J}_\ell(a,r)$ is defined in (2.1).

This result, which is proven in Appendix A, allows us to establish the following lemma. (Note: In the bound above and in all similar bounds in this paper, we abuse the notation slightly for $\ell = 0$, in which case the expression on the left-hand side is assumed to be bounded.)

LEMMA 2.2. *For any $m \in L^\infty$,*

$$\|K - K^M\|_\infty \to 0$$

as $M \to \infty$, where the operator norm is the one induced by the L^∞-norm.

Proof. Let $u \in L^\infty$. Then

$$\int_0^{2\pi} |m(r,\theta)u(r,\theta)e^{-i\ell\theta}|d\theta \le 2\pi\|m\|_\infty\|u\|_\infty.$$

Hence, for $M \ge 0$,

$$\begin{aligned}\|(K - K^M)u\|_\infty &\le \frac{\pi\kappa^2}{2}\|m\|_\infty\|u\|_\infty \sum_{|\ell|>M} \left\| \int_{R_0}^{R_1} |\mathcal{J}_\ell(a,r)|r\,dr \right\|_\infty \\ &= \mathcal{O}\left(\sum_{|\ell|>M} \frac{1}{\ell^2} \right) \|u\|_\infty \\ &= \mathcal{O}(M^{-1})\|u\|_\infty.\end{aligned}$$

Therefore, $\|K - K^M\|_\infty = \mathcal{O}(M^{-1}) \to 0$ as $M \to \infty$. ∎

Remark 2.3. The following proof of the existence and uniform boundedness of $(I-K^M)^{-1}$ depends crucially on the existence and boundedness of $(I-K)^{-1}$. By the Riesz–Fredholm theory (see, for example, [20, p. 29]), since K is a compact operator on L^∞, $(I-K)^{-1}$ exists and is bounded if $I-K$ is injective. The injectivity of this operator is equivalent to the uniqueness of solutions of the corresponding Helmholtz equation (1.2). The uniqueness result relevant for our setting follows from corresponding (more general) results for acoustic scattering proved in [30] under assumptions that we state more precisely below with the help of the following definitions.

DEFINITION 2.4. *Given a compact set $D \subset \mathbb{R}^n$, we say that a function f has piecewise continuous derivatives of order k on D, denoted by $f \in C^k_{pw}(D)$, if and only if there exist a finite number of open, disjoint subsets of D, denoted by $D_1, D_2, \dots, D_p$, such that $D = \bigcup_{i=1}^p \overline{D_i}$ and there exist functions $f_i \in C^k(\overline{D_i})$ such that $f|_{D_i} = f_i|_{D_i}$. In an entirely analogous fashion we define spaces of functions with piecewise-Hölder continuous derivatives of order k on D, denoted by $C^{k,\alpha}_{pw}(D)$.*

DEFINITION 2.5. *We say that the scattering inhomogeneity m belongs to $\mathcal{M}$ if and only if* (1) *$m \in C^{0,\alpha}_{pw}(D)$ for some compact set D that properly contains the support of m and* (2) *each of the corresponding subsets $D_1, D_2, \dots, D_p$, as defined in Definition* 2.4*, has a Lipschitz boundary.*

Remark 2.6. With these definitions, we can state the unique solvability result for (1.5), which is based on the uniqueness result of [30], more precisely: $I-K$ admits a bounded inverse on L^∞ for each $m \in \mathcal{M}$. Hence, throughout this paper, we will assume that $m \in \mathcal{M}$. Note that the uniqueness result of [30] makes use of a unique continuation result due to Heinz [13], which assumes C^1 boundary regularity of the subsets D_i defined above. However, more recent unique continuation results make much weaker assumptions (see [19] and the references therein) and hence allow us

to relax the C^1 regularity assumption to Lipschitz regularity (which suffices to allow integration by parts in obtaining the appropriate weak formulation).

We can now establish the following theorem.

THEOREM 2.7. *Given $m \in \mathcal{M}$, for M sufficiently large the operators $(I-K^M)^{-1}$ exist on L^∞ and are uniformly bounded. Thus, given any incident field u^i, (2.3) admits a unique solution $v \in L^\infty$ for all M sufficiently large.*

Proof. Since, by the discussion above, $I-K$ has a bounded inverse, Lemma 2.2 and [20, Theorem 10.1, p. 142] imply that for all sufficiently large M the inverse operators $(I-K^M)^{-1}$ exist and are uniformly bounded. ∎

3. Error bounds. The approximate integral equation (2.3) was obtained by truncating the Fourier series of both the incident field u^i and the integral operator K at each radius; as mentioned above, the exact solution v of this approximate equation is to be viewed as an approximate solution of the exact equation (1.5). As it happens, the function v is a *higher-order approximation* of the exact solution u of (1.5). Roughly speaking, this result follows from the fact that the integral operator Ku and the incident field u^i are smooth and periodic functions of the angular variable, which are thus approximated to higher-order by their truncated Fourier series.

In this section we derive bounds on the error implicit in the approximation of u by v. Of course the full numerical implementation of the method introduces additional errors (e.g., errors arising from radial numerical quadratures), but here we study the accuracy with which v approximates the exact solution u only. Higher-order methods for computing the required radial integrals are discussed in [5, 7, 8, 14].

3.1. Error in approximated Fourier modes. The error in the solution v^M of the approximate integral equation (2.3) at a point $x=(a,\phi)\in\mathbb{R}^2$ is given by

$$|u(x)-v^M(x)| \le |(u-u^M)(x)| + |u^M(x)-v^M(x)|, \tag{3.1}$$

where $(u-u^M)$ is the "tail" of the Fourier series of u,

$$(u-u^M)(a,\phi) = \sum_{|\ell|>M} u_\ell(a)e^{i\ell\phi}.$$

In this section, we derive a bound on the second term on the right-hand side of (3.1).

Subtracting the identities (see (2.6))

$$\begin{aligned} u^M &= u^{i,M} + K^M u, \\ v^M &= u^{i,M} + K^M v^M, \end{aligned}$$

we obtain

$$\begin{aligned} u^M - v^M &= K^M(u-v^M) \\ &= K^M(u^M-v^M) + K^M(u-u^M). \end{aligned}$$

In view of Theorem 2.7 and calling

$$\varepsilon_M = \|u^M - v^M\|_\infty, \tag{3.2}$$

we obtain

$$\varepsilon_M \le B\|K^M(u-u^M)\|_\infty$$

for sufficiently large M, where B is a uniform bound on $\|(I - K^M)^{-1}\|$.

To bound $K^M(u - u^M)$, we note that

$$\|K^M(u - u^M)\|_\infty \leq \sum_{\ell=-M}^{M} \|K_\ell(u - u^M)\|_\infty$$

and

$$\int_0^{2\pi} m(r,\theta)(u - u^M)(r,\theta)e^{-i\ell\theta}d\theta = 2\pi \sum_{|j|>M} m_{\ell-j}(r)u_j(r).$$

Therefore, by Lemma 2.1,

$$\|K_\ell(u - u^M)\|_\infty \leq \frac{C}{\ell^2} \sum_{|j|>M} \|m_{\ell-j}\|_\infty \|u_j\|_\infty. \tag{3.3}$$

We will bound this expression through consideration of bounds on the Fourier coefficients of m and u. To this end, we make use of the following lemma, which is a slight variation of a classical result [34, pp. 48, 71] and can be proved by multiple integrations by parts.

LEMMA 3.1. *If g is a 2π-periodic function such that $g \in C^k([0, 2\pi])$ with $g^{(n)}(0) = g^{(n)}(2\pi)$ for $n = 0, \ldots, k$, and $g^{(k+1)}$ is of bounded variation, then the Fourier coefficients c_ℓ of g satisfy $|c_\ell| \leq C|\ell|^{-(k+2)}$ for some constant C. If $g^{(1)}$ is of bounded variation on $[0, 2\pi]$, then $|c_\ell| \leq C|\ell|^{-1}$.*

The following useful theorem describes the dependence of the regularity of u on the regularity of m. Variations on the results for the Newtonian potential (see [2, p. 223], [11, pp. 78–80], and [12, pp. 53, 56]) give us the following result.

THEOREM 3.2. *Let D be an open set which properly contains the compact support of $m \in \mathcal{M}$, and let u be the solution of (1.5) on D for a given incident field u^i. Then $u \in C^{1,\alpha}(D)$. Furthermore, if Ω is an open subset of D and $m \in C^{k,\alpha}(\Omega)$, then $u \in C^{k+2,\alpha}(\Omega)$.*

Remark 3.3. Since Ω is an arbitrary bounded, open set, this theorem relates the *local* regularity of u to the *local* regularity of m.

To bound the discrete convolution in (3.3) we also need results on the decay rates of the Fourier coefficients of m and u.

LEMMA 3.4. *Let $m \in \mathcal{M}$. Define the annular region $A = \{(a, \phi) : 0 \leq R_0 \leq a \leq R_1\}$ such that A properly contains the support of m. If $m \in C^{k,\alpha}(A) \cap C^{k+2}_{pw}(A)$ for $k \geq 0$, then the Fourier coefficients of the total field u satisfy*

$$\|u_\ell\|_\infty \leq \frac{C}{|\ell|^{k+4}}.$$

If $m \in C^1_{pw}(A)$, then the Fourier coefficients of the total field u satisfy

$$\|u_\ell\|_\infty \leq \frac{C}{|\ell|^3}.$$

Proof. From (2.2), we see that the coefficients in the Fourier series representation of (1.5) are given by

$$u_\ell(a) = u^i_\ell(a) - \frac{i\pi\kappa^2}{2} \int_{R_0}^{R_1} \mathcal{J}_\ell(a, r)(mu)_\ell(r)r\, dr.$$

Since $m \in C^{k,\alpha}(A) \cap C^{k+2}_{pw}(A)$, Theorem 3.2 implies that $u \in C^{k+2,\alpha}(A)$ and hence, $mu \in C^{k,\alpha}(A) \cap C^{k+2}_{pw}(A)$. Therefore, by Lemma 3.1, the Fourier coefficients of mu satisfy

$$\|(mu)_\ell\|_\infty \leq \frac{C_1}{|\ell|^{k+2}}.$$

Again by Theorem 3.2, since u^i solves the homogeneous Helmholtz equation (1.3), $u^i \in C^\infty(\mathbb{R}^2)$. Thus, the Fourier coefficients u^i_ℓ decay faster than $|\ell|^{-p}$ for any positive integer p as $\ell \to \infty$. Therefore, by Lemma 2.1, we obtain

$$\begin{aligned}\|u_\ell\|_\infty &\leq \frac{C_2}{\ell^2}\frac{C_1}{|\ell|^{k+2}} \\ &\leq \frac{C}{|\ell|^{k+4}}.\end{aligned}$$

The proof for $m \in C^1_{pw}$ is similar. ∎

We can now establish the main result of this paper.

THEOREM 3.5. *Let $m \in \mathcal{M}$. Define the annular region $A = \{(a,\phi) : 0 \leq R_0 \leq a \leq R_1\}$ such that A properly contains the support of m.*

If $m \in C^1_{pw}(A)$, then as $M \to \infty$

$$\varepsilon_M = \|u^M - v^M\| \leq B\|K^M(u - u^M)\| = \mathcal{O}\left(\frac{1}{M^3}\right).$$

If $m \in C^{0,\alpha}(A) \cap C^2_{pw}(A)$, then as $M \to \infty$

$$\varepsilon_M = \mathcal{O}\left(\frac{1}{M^5}\right).$$

If $m \in C^{k,\alpha}(A) \cap C^{k+2}_{pw}(A)$ for $k \geq 1$, then as $M \to \infty$

$$\varepsilon_M = \mathcal{O}\left(\frac{1}{M^{k+6}}\right).$$

Proof. We seek a bound on $\|K^M(u - u^M)\|_\infty \leq \sum_{\ell=-M}^{M} \|K_\ell(u - u^M)\|_\infty$. By Lemma 3.4, we obtain

$$\begin{aligned}\|K_\ell(u - u^M)\|_\infty &\leq \frac{C_1}{\ell^2} \sum_{|j|>M} \frac{1}{|\ell - j|^{k+2}} \frac{1}{|j|^{k+4}} \\ &= \frac{C_1}{\ell^2} \sum_{j>M} \frac{1}{j^{k+4}} \left(\frac{1}{(j-\ell)^{k+2}} + \frac{1}{(j+\ell)^{k+2}}\right) \\ &\leq \frac{2C_1}{\ell^2} \sum_{j>M} \frac{1}{j^{k+4}} \frac{1}{(j - |\ell|)^{k+2}}\end{aligned}$$

for $\ell = -M, \ldots, M$. This expression also holds for $m \in C^{1,\alpha}_{pw}(A)$ with $k = -1$. Clearly, it suffices to bound $\|K_\ell(u - u^M)\|_\infty$ for $\ell = 0, \ldots, M$.

Thus, for $k \geq 0$, we obtain

$$\sum_{j>M} \frac{1}{j^{k+4}} \frac{1}{(j-\ell)^{k+2}} \leq \frac{1}{M^{k+4}} \frac{C_2}{(M+1-\ell)^{k+1}}.$$

For $k = -1 (m \in C^{1,\alpha}_{pw}(A))$, on the other hand, we find that

$$\begin{aligned}\sum_{j>M} \frac{1}{j^3}\frac{1}{j-\ell} &\le \frac{1}{M^2}\frac{1}{\ell}\sum_{j>M}\left(\frac{1}{j-\ell}-\frac{1}{j}\right)\\ &\le \frac{1}{M^2}\frac{C_3}{\ell}\log\left(\frac{M+1}{M+1-\ell}\right)\\ &\le \frac{1}{M^2}\frac{C_3}{M+1-\ell},\end{aligned}$$

since $\log x \le x-1$ for $x>0$.

To obtain the final result, it suffices to consider sums of the following form:

$$\sum_{\ell=1}^{M}\frac{1}{\ell^2}\frac{1}{(M+1-\ell)^p}$$

for $p = 1, 2, \ldots$. First, for $p \ge 2$,

$$\begin{aligned}\sum_{\ell=1}^{M}\frac{1}{\ell^2}\frac{1}{(M+1-\ell)^p} &\le \sum_{\ell=1}^{M}\frac{1}{\ell^2}\frac{1}{(M+1-\ell)^2}\\ &\le 2\sum_{\ell=1}^{\lceil \frac{M}{2}\rceil}\frac{1}{\ell^2}\frac{1}{(M+1-\ell)^2}\\ &= \mathcal{O}\left(\frac{1}{M^2}\right)\end{aligned}$$

as $M \to \infty$. Finally, for $p = 1$, we obtain

$$\begin{aligned}\sum_{\ell=1}^{M}\frac{1}{\ell^2}\frac{1}{M+1-\ell} &= \sum_{\ell=1}^{\lceil \frac{M}{2}\rceil}\frac{1}{\ell^2}\frac{1}{M+1-\ell} + \sum_{\ell=\lceil \frac{M}{2}\rceil+1}^{M}\frac{1}{\ell^2}\frac{1}{M+1-\ell}\\ &= \mathcal{O}\left(\frac{1}{M}\right)+\mathcal{O}\left(\frac{\log M}{M^2}\right)\\ &= \mathcal{O}\left(\frac{1}{M}\right)\end{aligned}$$

as $M \to \infty$. Combining these results, the theorem follows. ∎

Remark 3.6. Of course, there are many other conditions on m for which the corresponding convergence rates could be determined; for instance, one might remove the requirement of Hölder continuity. In every case, the convergence rates are directly determined by the rate of decay of the Fourier coefficients of m and u. We do not attempt to provide a comprehensive listing of all possible regularity conditions and their corresponding convergence rates.

Remark 3.7. Numerical experiments indicate that the bounds of Theorem 3.5 are tight. The resulting convergence rates depend on k in a particularly interesting way. As we have shown, the method exhibits *third-order* convergence for $m \in C^1_{pw}(A)$, *fifth-order* convergence for $m \in C^{0,\alpha}(A) \cap C^2_{pw}(A)$, and *seventh-order* convergence for $m \in C^{1,\alpha}(A) \cap C^3_{pw}(A)$. This rather interesting and unexpected k-dependence of the convergence rates is observed in the numerical examples of section 5.

3.2. Total error in the interior and exterior fields. Up to this point, we have computed only convergence rates for the approximated modes, i.e., the modes of order ℓ with $|\ell| \leq M$. Given these convergence rates, we can now easily estimate the total error. We make a distinction here between two types of error: the *interior field error* (the error on the domain of integration $A = \{(a, \phi) : 0 \leq R_0 \leq a \leq R_1\}$) and the *exterior field error* (the error outside of A). The interior field error is simply the difference between the true solution $u(x)$ and the solution $v^M(x)$ of (2.3) on A. Clearly, on A we have

$$\begin{aligned}\|u - v^M\|_\infty &\leq \|u^M - v^M\|_\infty + \|u - u^M\|_\infty \\ &\leq \varepsilon_M + \tau_M,\end{aligned}$$

where ε_M is defined in (3.2) and $\tau_M = \|u - u^M\|_\infty$.

Remark 3.8. Note that the decay rate of $(u - u^M)(x_0)$ for a particular point $x_0 \in A$, as opposed to the maximum error in all of A, depends on the regularity of m in a neighborhood of the circle with radius $r_0 = |x_0|$ centered at the origin. Hence, in general, the convergence rate of $v^M(x_0)$ to $u(x_0)$ may vary with the choice of $x_0 \in A$. In particular, the regularity of m in a neighborhood of the circle with radius $r_0 = |x_0|$ centered at the origin determines the regularity of u in that neighborhood and hence also determines the decay rate of the Fourier coefficients $u_\ell(r_0)$. This decay rate in turn determines whether ε_M or $(u - u^M)(x_0)$ dominates the convergence rate. The pointwise convergence rate is of limited usefulness, however; the following corollary to Theorem 3.5 provides a bound on the maximum error in the computed interior field.

COROLLARY 3.9 (interior field error). *If $m \in C^{k,\alpha}(A) \cap C^{k+2}_{pw}(A)$, then the interior field error is given by*

$$\|u - v^M\|_\infty = \mathcal{O}\left(\frac{1}{M^{k+3}}\right).$$

This result holds with $k = -1$ for $m \in C^1_{pw}(A)$.

Proof. By Lemma 3.4,

$$\tau_M = \sum_{\ell > M} \frac{C}{\ell^{k+4}} = \mathcal{O}\left(\frac{1}{M^{k+3}}\right)$$

as $M \to \infty$. Clearly, by Theorem 3.5, τ_M dominates ε_M for every k. The proof for $m \in C^1_{pw}(A)$ is similar. ∎

Before discussing convergence rates in the exterior field, we describe how to extend the approximate solution v^M, which we have computed only on the interior of A, to the exterior field. Since the integration in (1.5) is performed only over the support of m, one can easily see that, given the solution u on the boundary of A, the solution in the rest of $\mathbb{R}^2$ can be computed simply by an appropriate scaling of the Fourier modes of u^s on the (circular) inner and outer boundaries of A at radii R_0 and R_1, respectively. More precisely, we find that

$$u^s_\ell(a) = \begin{cases} \dfrac{J_\ell(\kappa a)}{J_\ell(\kappa R_0)} u^s_\ell(R_0) & \text{if } 0 \leq a < R_0, \\ \dfrac{H^1_\ell(\kappa a)}{H^1_\ell(\kappa R_1)} u^s_\ell(R_1) & \text{if } a > R_1. \end{cases} \tag{3.4}$$

Our approximate solution v^M is extended to the exterior of A by the same procedure.

COROLLARY 3.10 (exterior field error). *Let $m \in \mathcal{M}$. Given $x_0 \notin A$, extend the approximate solution v^M to the exterior of A by means of* (3.4) *above. More precisely, for $\ell = -M, \ldots, M$, let $r_0 = |x_0|$ and define*

$$v_\ell(r_0) = u_\ell^i(r_0) + \begin{cases} \dfrac{J_\ell(\kappa r_0)}{J_\ell(\kappa R_0)}[v_\ell(R_0) - u_\ell^i(R_0)] & \text{if } 0 \le r_0 < R_0, \\ \dfrac{H_\ell^1(\kappa r_0)}{H_\ell^1(\kappa R_1)}[v_\ell(R_1) - u_\ell^i(R_1)] & \text{if } r_0 > R_1. \end{cases}$$

(Note: If $R_0 = 0$, then the integration domain is a disc and, hence, only the part of the equation above corresponding to $r_0 > R_1$ applies.) Then, the exterior field error at $x_0 \notin A$ is given by

$$|u(x_0) - v^M(x_0)| = \mathcal{O}(\varepsilon_M)$$

as $M \to \infty$, where ε_M, defined in (3.2)*, has bounds given by Theorem* 3.5.

Proof. Assume that $r_0 > R_1$; the proof for $0 \le r_0 < R_0$ is similar. Defining the scaling factors $\beta_\ell(r_0)$ at radius r_0 by

$$\beta_\ell(r_0) = \frac{H_\ell^1(\kappa r_0)}{H_\ell^1(\kappa R_1)}, \tag{3.5}$$

we have

$$\begin{aligned} |u(x_0) - v^M(x_0)| &\le \sum_{\ell=-M}^{M} |\beta_\ell(r_0)|\,|u_\ell(R_1) - v_\ell(R_1)| + |(u - u^M)(x_0)| \\ &\le \varepsilon_M \sum_{\ell=-M}^{M} |\beta_\ell(r_0)| + |(u - u^M)(x_0)|. \end{aligned}$$

As before, let S denote the circle of radius r_0 about the origin. Since $r_0 = |x_0| > R_1$, there exists a neighborhood $N(S)$ of S such that $m|_{N(S)} = 0$. Therefore, $u \in C^\infty(N(S))$ and $|(u - u^M)(x_0)| \le \frac{C}{M^p}$ for *any* integer $p > 0$. This implies that $|(u - u^M)(x_0)|$ is always dominated by ε_M.

Since the Hankel function $H_\ell^1(z) = J_\ell(z) + i\,Y_\ell(z)$, where $Y_\ell(z)$ is the Neumann function of order ℓ, we complete the proof by using the asymptotic expressions for J_ℓ and Y_ℓ [1, p. 365] for fixed z and as $\ell \to \infty$ through positive real values,

$$\begin{aligned} J_\ell(z) &\sim \frac{1}{\sqrt{2\pi\ell}} \left(\frac{ez}{2\ell}\right)^\ell, \\ Y_\ell(z) &\sim -\sqrt{\frac{2}{\pi\ell}} \left(\frac{ez}{2\ell}\right)^{-\ell}. \end{aligned}$$

Therefore, from these asymptotic expressions and from (3.5), we obtain

$$\begin{aligned} |\beta_\ell(r_0)|^2 &= \left|\frac{Y_\ell(\kappa r_0)}{Y_\ell(\kappa R_1)}\right|^2 \frac{1 + \left|\frac{J_\ell(\kappa r_0)}{Y_\ell(\kappa r_0)}\right|^2}{1 + \left|\frac{J_\ell(\kappa R_1)}{Y_\ell(\kappa R_1)}\right|^2} \\ &\sim \left(\frac{R_1}{r_0}\right)^{2\ell} \end{aligned}$$

as $\ell \to \infty$. This implies that $|\beta_\ell(r_0)|$ is summable. We conclude that as $M \to \infty$

$$|u(x_0) - v^M(x_0)| = \mathcal{O}(\varepsilon_M). \qquad \square$$

Note that while $u \in C^\infty$ on the exterior of A, this function may be much less regular on the interior of A (in general, $u \in C^{1,\alpha}$ for $m \in \mathcal{M}$). Hence, the decay of $u - u^M$ on the exterior of A is superalgebraic, whereas $u - u^M$ may decay as slowly as $\mathcal{O}(M^{-2})$ on the interior of A. This fact is responsible for the interesting result that the method converges more rapidly on the exterior of A than on the interior (where $u - u^M$ may dominate ε_M).

These remarks are particularly relevant in the evaluation of radar cross sections, an important measure in many applications. The evaluation of radar cross sections requires the computation of the *far field*. Although Corollary 3.10 does not directly address the error in the far field, we obtain an approximate far field by a scaling of the Fourier modes of v^M just as in the computation of the exterior field. As in [4, p. 6], we define the far field, u_∞, by the asymptotic representation of the scattered field as $r \to \infty$, i.e.,

$$u^s(r,\phi) = e^{i(\kappa r - \frac{\pi}{4})}\sqrt{\frac{2}{\pi\kappa r}}[u_\infty(\phi) + \mathcal{O}(r^{-1})].$$

From (3.4) and the asymptotic expression for $H^1_\ell(z)$ for fixed ℓ as $z \to \infty$ [1, p. 364], we obtain the Fourier modes of u_∞ by a simple scaling of the Fourier modes of u^s:

$$(u_\infty)_\ell = \frac{u^s_\ell(R_1)}{i^\ell H^1_\ell(\kappa R_1)}.$$

If we define the approximate far field v_∞ in the same way, we can prove that

$$\|u_\infty - v_\infty\| = \mathcal{O}(\varepsilon_M)$$

as $M \to \infty$. The proof of this fact is nearly identical to that of Corollary 3.10.

The predicted convergence rates in both the interior field and the far field are verified through several computational examples in section 5.

4. Computation of the angular integral. We have proven that the solution to the approximate integral equation (2.3) provides a higher-order approximation to the solution of the exact integral equation (1.5) for the scattering problem. However, to this point, we have not discussed any methods for computing the required angular and radial integrals. This paper primarily addresses the theoretical aspects of the method; for a discussion of a particular efficient, higher-order radial integrator, we refer to [5, 7, 8, 14]. On the other hand, with regards to the angular integrals, we show below that the Fourier coefficients of $m(r,\theta)v^M(r,\theta)$ can be computed efficiently and *exactly* (except for roundoff) by means of FFTs.

The required angular integrals are given by

$$I_\ell(r) = \int_0^{2\pi} m(r,\theta)v^M(r,\theta)e^{-i\ell\theta}d\theta, \tag{4.1}$$

where v^M solves the approximate integral equation (2.3). We can express this integral

in terms of the Fourier coefficients of m and v, i.e.,

$$\begin{aligned} I_\ell(r) &= \int_0^{2\pi} \left(\sum_{j=-\infty}^{\infty} m_j(r) e^{ij\theta} \right) \left(\sum_{k=-M}^{M} v_k(r) e^{ik\theta} \right) e^{-i\ell\theta} d\theta \\ &= 2\pi \sum_{k=-M}^{M} m_{\ell-k}(r) v_k(r), \end{aligned} \tag{4.2}$$

where $\ell = -M, \ldots, M$. Hence, we obtain a finite discrete convolution of Fourier coefficients of m and v at each radius; since $|\ell| \le M$ and $|k| \le M$, we have $|\ell - k| \le 2M$. Thus, as stated above, given the Fourier coefficients $m_\ell(r)$ for $|\ell| \le 2M$, we can compute the required angular integrals *exactly*. Furthermore, as is well known, such discrete convolutions may be evaluated (with no discretization error) with the help of FFTs [25, pp. 531–537] so that the computational cost at each radius is of the order of $M \log M$.

This method of computing the angular integrals has an interesting implication concerning the dependence of the solution u on the inhomogeneity m. Indeed, since the computation involves only modes m_ℓ, $|\ell| \le 2M$, replacing m with m^{2M} in the integral equation yields no additional error, i.e.,

$$I_\ell(r) = \int_0^{2\pi} m^{2M}(r,\theta) v^M(r,\theta) e^{-i\ell\theta} d\theta. \tag{4.3}$$

Hence, in a sense, the truncation of the Fourier series of the integral operator *implies* an associated truncation of the Fourier series of the refractive index—as a result of the band-limited nature of the solution v^M. Thus, surprisingly, the low-order approximation of a discontinuous refractive index at each radius by its truncated Fourier series yields *no additional error* beyond that of our original, higher-order truncation of the Fourier series of K. This points to the interesting cancellation of errors phenomenon mentioned briefly in the introduction: the large errors in the Fourier approximation of the refractive index *cancel* in the discrete integration process yielding small errors—high-order accurate approximations—in the evaluation of $I_\ell(r)$.

Note that the discrete-convolution approach to the evaluation of $I_\ell(r)$ ($\ell = -M, \ldots, M$) is equivalent to trapezoidal rule integration of (4.3) with a sufficiently large number of integration points N_θ. This follows from the fact that the trapezoidal rule with N_θ points on the interval $[0, 2\pi]$ integrates the Fourier modes $e^{ik\theta}$ for $|k| < N_\theta$ exactly: using N_θ points in the trapezoidal rule to approximate $\int_0^{2\pi} e^{ik\theta} d\theta$, we obtain

$$\frac{2\pi}{N_\theta} \sum_{j=0}^{N_\theta - 1} e^{2\pi i j k / N_\theta} = \begin{cases} 2\pi & \text{if } k = pN_\theta \text{ for } p \in \mathbb{Z}, \\ 0 & \text{otherwise.} \end{cases}$$

Therefore, since the largest mode in the integrand of (4.3) is $2M + M + M = 4M$, if we choose $N_\theta = cM$, where $c > 4$, the trapezoidal rule computes (4.3) exactly (except for roundoff) and the use of FFTs yields a complexity of $\mathcal{O}(M \log M)$. Algorithmically, this is entirely equivalent to computing the discrete convolution (4.2) using FFTs.

5. Computational examples. In this section, we illustrate the performance of the two-dimensional algorithm for a variety of scattering configurations. We first study the convergence of the method for two scatterers for which analytical solutions

are known. We then verify that the algorithm achieves the predicted convergence rates for three scatterers of varying degrees of regularity.

In each case, we compute the near and far fields produced under plane wave incidence, $u^i(x,y) = e^{i\kappa x}$. To compute the maximum error in the near field, we evaluate the solution computed by our method on an evenly spaced polar grid. On this grid, we evaluate the maximum absolute error as compared with either the analytical solution (when it is available) or the solution computed with a finer discretization. The maximum error in the far field is computed similarly by interpolating to an evenly spaced angular grid.

The results for each example are given in the accompanying figures and tables. The figures include visualizations of $-m(x) = n^2(x) - 1$ and the computed near field intensity, $|v^M|^2$. The tables provide values for the number of modes M in the approximate solution v^M, the wall-clock time required, and the maximum absolute errors in the near and far field denoted by ϵ_u^{nf} and ϵ_u^{ff}, respectively. Additionally, the ratios of the errors at successive levels of discretization are listed to illustrate the convergence rates. For some discretizations, the accuracy in the computed solution has reached either machine-precision accuracy (actually just less than machine precision due to round-off errors), the accuracy of the radial integration, or the tolerance of the linear solver. In such a case, we observe no improvement in the error of the solution as we refine the discretization and hence, to indicate a converged solution, we write "Conv." in the ratio column.

Our main goal in this section is to verify the convergence rates established in Theorem 3.5 and Corollaries 3.9 and 3.10. Hence, in this section, we are primarily concerned with the convergence in the number of Fourier modes M, rather than the convergence in the number of radial points. We also seek to demonstrate the $\mathcal{O}(M \log M)$ complexity of the angular integration method. We therefore fix the number of radial points at a sufficiently large value and we hold the number of iterations of the linear solver (GMRES) fixed at a value that produces a sufficiently accurate solution of the linear system. This isolates the dependence of the times and errors on M and allows us to confirm the computational complexity and the predicted convergence rates. All of these results were computed using a 700 MHz Pentium III Xeon workstation.

We first compute the scattering by two obstacles for which an analytical solution is known: (1) a cylindrically symmetric scatterer centered at the origin with piecewise-constant refractive index and (2) a disc centered at $(1\lambda, 0)$ with constant refractive index.

The results for the first example are presented in Figure 5.1 and Table 5.1. Here the inner disc has a radius equal to 1λ and a refractive index $n = 2$; the outer annulus has an outer radius of 2λ and a refractive index $n = 3$. Thus, this scatterer has a diameter of 10 interior wavelengths. (Perhaps the best indication of the difficulty of a scattering problem is given by the size of the scatterer in terms of interior wavelengths, since the numerical method must resolve these wavelengths to provide any accuracy.) One may also observe that the method obtains an exponential convergence rate. This occurs despite the discontinuity in the refractive index because, at each radius, the refractive index is a C^∞ function of the angular variable. Finally, we observe that the time required is consistent with an $\mathcal{O}(M \log M)$ complexity.

The results for the second example are presented in Figure 5.2 and Table 5.2. Here the disc is centered at $(1\lambda, 0)$ and has a diameter of 1λ and a refractive index $n = \sqrt{2}$. Thus, it has a diameter of $\sqrt{2}$ interior wavelengths. As opposed to the previous

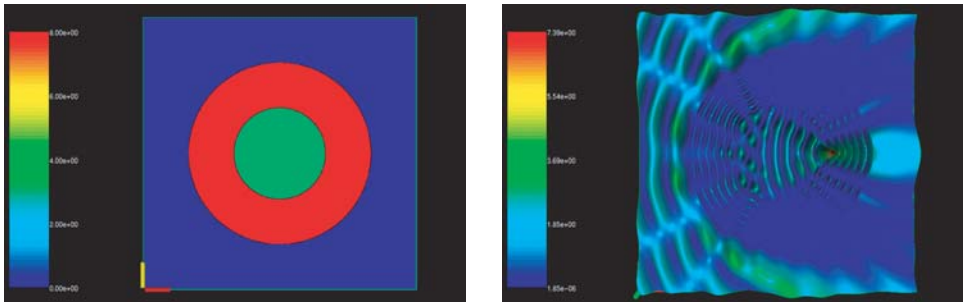

(a) Scatterer ($-m = n^2 - 1$) (b) Near Field Intensity ($|u|^2$)

FIG. 5.1. *Visualizations for a radially layered scatterer. Diameter* = 10 *interior wavelengths.*

TABLE 5.1
Convergence rate for a radially layered scatterer. Diameter = 10 *interior wavelengths.*

M	Time	ϵ_u^{nf}	Ratio	ϵ_u^{ff}	Ratio
15	3.05s	8.50e-2		4.28e-2	
30	3.83s	1.13e-9	7.52e+7	5.46e-13	7.83e+10
60	5.46s	1.68e-12	6.73e+2	4.97e-13	Conv.

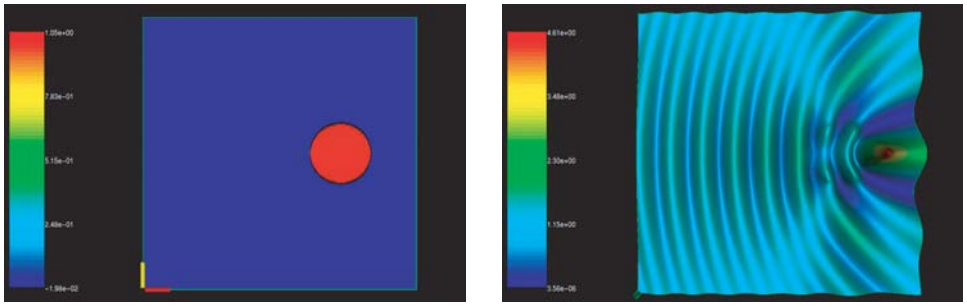

(a) Scatterer ($-m = n^2 - 1$) (b) Near Field Intensity ($|u|^2$)

FIG. 5.2. *Visualizations for an off-center disc. Diameter* = $\sqrt{2}$ *interior wavelengths.*

TABLE 5.2
Convergence for an off-center disc. Diameter = $\sqrt{2}$ *interior wavelengths.*

M	Time	ϵ_u^{nf}	Ratio	ϵ_u^{ff}	Ratio
15	7s	6.22e-2			
30	13s	5.95e-3	10.45	1.58e-3	18.80
60	25s	1.13e-3	5.27	1.83e-4	8.63
120	49s	2.83e-4	3.99	2.27e-5	8.06
240	99s	5.99e-5	4.72	2.84e-6	7.99
480	194s	6.65e-6	9.01	3.56e-7	7.98
960	386s	1.99e-6	3.34	4.42e-8	8.05
1920	808s	2.75e-7	7.24	4.21e-9	10.50

example, however, we do not observe an exponential rate of convergence despite the fact that the disc has a constant refractive index. Since the disc is not centered at the origin, the refractive index at each radius is actually a *discontinuous* function of

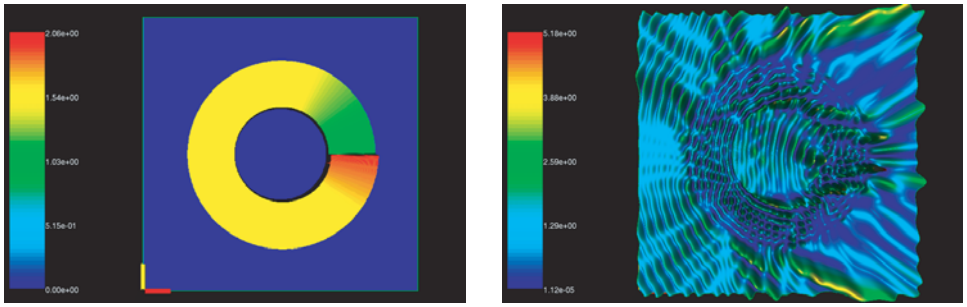

(a) Scatterer ($-m = n^2 - 1$) (b) Near Field Intensity ($|u|^2$)

FIG. 5.3. *Visualizations for a discontinuous scatterer. Annulus thickness* ≈ 4.33 *interior wavelengths.*

TABLE 5.3
Convergence rate for a discontinuous scatterer. Annulus thickness ≈ 4.33 *interior wavelengths.*

M	Time	ϵ_u^{nf}	Ratio	ϵ_u^{ff}	Ratio
60	27s	3.24e-2		2.07e-2	
120	52s	4.69e-3	6.91	1.95e-3	10.62
240	109s	6.23e-4	7.53	2.32e-4	8.41
480	228s	9.71e-5	6.42	2.87e-5	8.08
960	458s	1.04e-5	9.34	3.53e-6	8.13
1920	898s	1.45e-6	7.17	3.83e-7	9.22

the angular variable. Since the analytical solution in this case is known, the off-center disc provides direct verification of the predicted convergence rates for a *discontinuous* refractive index. The table shows excellent agreement with the predicted third-order convergence in the far field. The convergence in the near field is less steady, but is consistent with the predicted second-order convergence in the near field. As in the previous example, we observe that the computing time scales appropriately with M.

We now illustrate the convergence of the method for a series of three simple scatterers of increasing degrees of regularity. In each case, $m(x) = 1 - n^2(x)$ is given in the following form:

$$m(r,\theta) = \begin{cases} -\frac{3}{2} - \frac{1}{2\pi} \sum_{|\ell|\geq 1} \left(\frac{i}{\ell}\right)^{k+2} e^{i\ell\theta} & \text{for } \frac{5}{2}\lambda \leq r \leq 5\lambda, \\ 0 & \text{otherwise.} \end{cases}$$

Note that for each integer k, this series becomes either a sine or cosine series with real coefficients. If $k = -1$, m is discontinuous and piecewise smooth as a function of θ. Further, for any integer $k \geq 0$, $m \in C^{k,\alpha} \cap C^{\infty}_{pw}$ as a function of θ. The three examples that follow illustrate the convergence of the method for $k = -1, 0, 1$. Because these scatterers are fully inhomogeneous, their size in terms of interior wavelengths is not easily defined. Note, however, that each annular scatterer has a radial thickness of 2.5λ in terms of incident wavelengths; if the refractive index were constant within the annulus and equal to the maximum, then the radial thickness of the annulus would be approximately 4.33, 4.15, and 4.54 interior wavelengths for $k = -1, 0, 1$, respectively.

The results for $k = -1$ are found in Figure 5.3 and Table 5.3. The predicted second-order convergence in the near field is exceeded and the third-order convergence

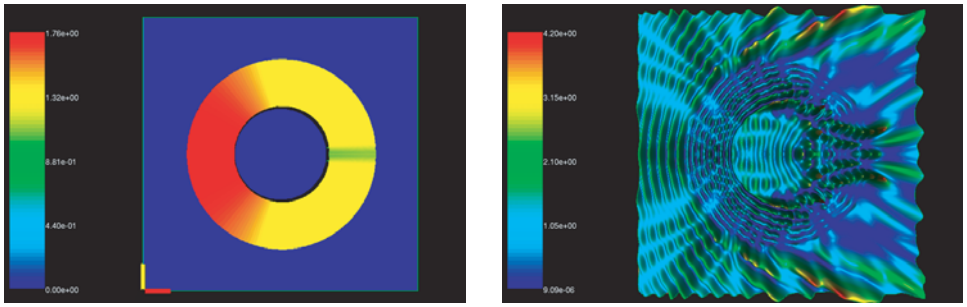

(a) Scatterer ($-m = n^2 - 1$) (b) Near Field Intensity ($|u|^2$)

FIG. 5.4. *Visualizations for a $C^{0,\alpha}$ scatterer. Annulus thickness ≈ 4.15 interior wavelengths.*

TABLE 5.4
Convergence rate for a $C^{0,\alpha}$ scatterer. Annulus thickness ≈ 4.15 interior wavelengths.

M	Time	ϵ_u^{nf}	Ratio	ϵ_u^{ff}	Ratio
60	23s	9.33e-4		7.06e-6	
120	50s	8.91e-5	10.47	1.30e-7	54.31
240	105s	1.15e-5	7.75	3.86e-9	33.68
480	212s	1.46e-6	7.88	1.17e-10	32.99
960	565s	1.83e-7	7.97	1.73e-11	Conv.
1920	1136s	1.98e-8	9.24	1.85e-11	Conv.

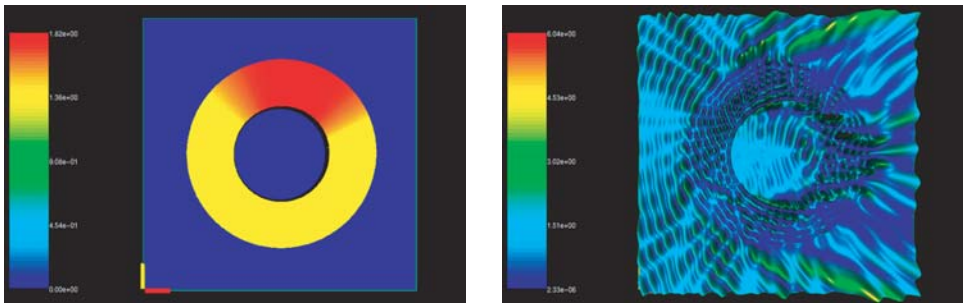

(a) Scatterer ($-m = n^2 - 1$) (b) Near Field Intensity ($|u|^2$)

FIG. 5.5. *Visualizations for a $C^{1,\alpha}$ scatterer. Annulus thickness ≈ 4.55 interior wavelengths.*

TABLE 5.5
Convergence rate for a $C^{1,\alpha}$ scatterer. Annulus thickness ≈ 4.55 interior wavelengths.

M	Time	ϵ_u^{nf}	Ratio	ϵ_u^{ff}	Ratio
60	36s	2.16e-5		7.33e-9	
120	72s	4.81e-7	44.91	1.06e-11	691.51
240	160s	1.05e-8	45.81	4.50e-12	Conv.
480	331s	4.76e-10	22.06	4.52e-12	Conv.
960	561s	1.36e-11	35.0	4.61e-12	Conv.
1920	1172s	1.94e-12	Conv.	4.72e-12	Conv.

in the far field is readily observed. The results of $k = 0$ are found in Figure 5.4 and Table 5.4. In this case, the predicted third-order convergence in the near field and

fifth-order convergence in the far field are both matched quite precisely. This example clearly illustrates the interesting jump in the far field convergence rate from third-order for a discontinuous refractive index to *fifth-order* for a $C^{0,\alpha}$ refractive index. Finally, the results for $k = 1$ are found in Figure 5.5 and Table 5.5. In this case, the predicted fourth- and seventh-order convergence rates in the near and far fields, respectively, are clearly exceeded. However, because convergence is so rapid, it is difficult to observe a definite pattern, especially in the far field convergence. In each of these cases, we note that the computing time scales appropriately with M. Finally, we mention that even the largest of these examples required less than 20 minutes and less than 700 MB of memory.

Appendix A. Bound on Fourier coefficients of the fundamental solution. To prove that solutions to the approximate integral equation (2.3) exist and to bound the convergence rate of the method, we need a bound on the decay rate of the Fourier coefficients of the fundamental solution $\mathcal{J}_\ell(a, r)$ defined in (2.1). This decay rate is given in Lemma 2.1.

According to [1, p. 362], for all integers $\ell \geq 0$ and for any real, nonnegative z,

$$|J_\ell(z)| \leq \frac{1}{\ell!}\left(\frac{z}{2}\right)^\ell \leq \frac{z^\ell}{\ell!}. \tag{A.1}$$

The following lemma provides a similar bound for $|Y_\ell(z)|$.

LEMMA A.1. *Let $z \in \mathbb{R}$ with $0 \leq z \leq R$. For all integers $\ell \geq 1$,*

$$|Y_\ell(z)| \leq C\frac{(\ell-1)!}{z^\ell},$$

and for $\ell = 0$,

$$|Y_\ell(z)| \leq C|\log(z)|,$$

where $C > 0$ depends only on R.

Proof. By [4, p. 51], $Y_\ell(z)$ is given for any nonnegative integer ℓ by

$$\begin{aligned} Y_\ell(z) = {} & \frac{2}{\pi}J_\ell(z)\log\left(\frac{z}{2}\right) - \frac{1}{\pi}\sum_{k=0}^{\ell-1}\frac{(\ell-k-1)!}{k!}\left(\frac{z}{2}\right)^{2k-\ell} \\ & -\frac{1}{\pi}\sum_{k=0}^{\infty}\frac{\psi(\ell+k)+\psi(k)}{(-1)^k k!(k+\ell)!}\left(\frac{z}{2}\right)^{2k+\ell}, \end{aligned} \tag{A.2}$$

where $\psi(0) = -\gamma \approx -0.5772$ and $\psi(k) = -\gamma + \sum_{j=1}^{k}\frac{1}{j}$ for $k \geq 1$.

To bound the second term in (A.2), we find that

$$\begin{aligned} \sum_{k=0}^{\ell-1}\frac{(\ell-k-1)!}{k!}\left(\frac{z}{2}\right)^{2k} &\leq (\ell-1)!\sum_{k=0}^{\infty}\frac{1}{k!}\left[\left(\frac{z}{2}\right)^2\right]^k \\ &\leq (\ell-1)!\, e^{\left(\frac{R}{2}\right)^2} \leq C_1(R)(\ell-1)!. \end{aligned}$$

Now note that for $k \geq 1$, $|\psi(0)| \leq 1$ and $0 \leq \psi(k) \leq -\gamma + k \leq k$.

Hence, for a bound on the third term in (A.2), we obtain

$$\sum_{k=0}^{\infty}\frac{|\psi(\ell+k)+\psi(k)|}{k!(k+\ell)!}\left(\frac{z}{2}\right)^{2k+\ell} \leq 2\sum_{k=0}^{\infty}\frac{1}{k!}\frac{[(R/2)^2]^{\frac{\ell}{2}+k}}{(\ell+k-1)!} \leq C_2(R),$$

since

$$\frac{[(R/2)^2]^{\frac{\ell}{2}+k}}{(\ell+k-1)!} \le C_3(R).$$

These bounds together with (A.1) yield the desired result. ∎

We now turn to the proof of the main lemma.

Proof of Lemma 2.1. First note that

$$\begin{aligned}\int_{R_0}^{R_1} |\mathcal{J}_\ell(a,r)|r\,dr &= |H_\ell^1(\kappa a)| \int_{R_0}^{a} |J_\ell(\kappa r)|r\,dr + |J_\ell(\kappa a)| \int_a^{R_1} |H_\ell^1(\kappa r)|r\,dr \\ &\le |J_\ell(\kappa a)| \int_{R_0}^{R_1} |J_\ell(\kappa r)|r\,dr + |J_\ell(\kappa a)| \int_a^{R_1} |Y_\ell(\kappa r)|r\,dr \\ &\quad + |Y_\ell(\kappa a)| \int_{R_0}^{a} |J_\ell(\kappa r)|r\,dr \\ &\le I_{J,J} + I_{J,Y} + I_{Y,J},\end{aligned}$$

where

$$\begin{aligned}I_{J,J} &= |J_\ell(\kappa a)| \int_0^{R_1} |J_\ell(\kappa r)|r\,dr, \\ I_{J,Y} &= |J_\ell(\kappa a)| \int_a^{R_1} |Y_\ell(\kappa r)|r\,dr, \\ I_{Y,J} &= |Y_\ell(\kappa a)| \int_0^{a} |J_\ell(\kappa r)|r\,dr.\end{aligned}$$

Note that $|J_{-\ell}(z)| = |(-1)^\ell J_\ell(z)| = |J_\ell(z)|$ and similarly $|Y_{-\ell}(z)| = |Y_\ell(z)|$. Hence, it suffices to bound these integrals for $\ell \ge 0$.

Thus, for $\ell \ge 0$, by (A.1),

$$I_{J,J} \le \frac{1}{(\ell!)^2} R_1^2 (\kappa R_1)^{2l} \le \frac{C_{J,J}}{\ell^2},$$

where $C_{J,J} > 0$ depends only on κ and R_1. By (A.1) and Lemma A.1, we find that for $\ell > 2$,

$$\begin{aligned}I_{J,Y} &\le C \frac{(\kappa a)^\ell}{\ell!} \int_a^{R_1} \frac{(\ell-1)!}{(\kappa r)^\ell} r\,dr \\ &= C \frac{{R_1}^2}{\ell(\ell-2)} \left[\left(\frac{a}{R_1}\right)^2 - \left(\frac{a}{R_1}\right)^\ell \right] \le \frac{C_{J,Y}}{\ell^2}.\end{aligned}$$

A similar argument shows that $I_{J,Y}$ is also bounded for $\ell = 0, 1, 2$. Finally, for $\ell \ge 1$, we find that

$$\begin{aligned}I_{Y,J} &\le C \frac{(\ell-1)!}{(\kappa a)^\ell} \int_0^{a} \frac{(\kappa r)^\ell}{\ell!} r\,dr \\ &= \frac{a^2}{\ell(\ell+2)} \le \frac{C_{Y,J}}{\ell^2}.\end{aligned}$$

It is not difficult to show that this same bound holds for $\ell = 0$. ∎

TABLE B.1
Relative errors in trapezoidal rule integration.

N	Error	Ratio
1	2.5e-1	
2	9.5e-2	2.6
4	3.5e-2	2.7
8	1.3e-2	2.7
8192	4.2e-7	

(a) $\int_0^{1/2} \sqrt{x}dx \approx 0.2357$

N	Error	Ratio
1	4.8e-2	
2	1.2e-2	4.0
4	2.9e-3	4.1
8	7.4e-4	3.9
8192	7.0e-10	

(b) $\int_0^{\pi/4} e^{\cos^2 x}dx \approx 1.8009$

N	Error	Ratio
1	5.5e-1	
2	6.0e-2	9.2
4	3.1e-4	1.9e+2
8	7.2e-10	4.3e+5
16	2.1e-23	3.4e+13

(c) $\int_0^{\pi} e^{\cos^2 x}dx \approx 5.5084$

Appendix B. Higher-order integration via the trapezoidal rule. When used to integrate a smooth and periodic function over its period, the trapezoidal rule obtains a truly extraordinary convergence rate (see [21, section 9.4] and [29]). As with our numerical method, this convergence behavior is due to the rapid decay of the function's Fourier coefficients (see Lemma 3.1). Since this fact may yet be unfamiliar to some readers, we illustrate trapezoidal rule convergence through three simple, one-dimensional integrals.

In Table B.1, we give the relative errors obtained when computing the integrals of the functions $\sqrt{x}$ and $e^{\cos^2 x}$ by means of the trapezoidal rule with N points. In Table B.1(a), we observe less than second-order convergence when computing $\int_0^{1/2} \sqrt{x}dx$, which is a result of the singularity in its first derivative at the origin. Table B.1(b) shows second-order convergence when computing $\int_0^{\pi/4} e^{\cos^2 x}dx$, which agrees with the well-known convergence rate predicted for the trapezoidal rule when integrating C^2 functions. Finally, in Table B.1(c), we observe an *exponential* convergence rate when computing $\int_0^{\pi} e^{\cos^2 x}$, the same function integrated in Table B.1(b). Note that in this example a relative error of 7×10^{-10} is obtained with 8 points, whereas in Table B.1(b), 8192 points are required for similar accuracy. This extraordinary convergence rate results because we are integrating a *smooth and periodic function over its period*.

Acknowledgments. Color visualizations were generated with the VTK-based visualization tool Vizamrai, developed by Steven Smith at the Center for Applied Scientific Computing (CASC) at Lawrence Livermore National Laboratory. The authors also gratefully acknowledge the constructive suggestions of an anonymous referee.

REFERENCES

[1] M. ABRAMOWITZ AND I. A. STEGUN, EDS., *Handbook of Mathematical Functions with Formulas, Graphs, and Mathematical Tables*, Dover, New York, 1965.
[2] L. BERS, F. JOHN, AND M. SCHECHTER, *Partial Differential Equations*, John Wiley and Sons, New York, 1964.
[3] N. N. BOJARSKI, *The k-space formulation of the scattering problem in the time domain*, J. Opt. Soc. Amer., 72 (1982), pp. 570–584.
[4] J. J. BOWMAN, T. B. A. SENIOR, AND P. L. E. USLENGHI, EDS., *Electromagnetic and Acoustic Scattering by Simple Shapes*, North-Holland, Amsterdam, 1969.
[5] O. P. BRUNO AND E. M. HYDE, *An efficient, preconditioned, high-order solver for scattering by two-dimensional, inhomogeneous media*, J. Comput. Phys., 200 (2004), pp. 670–694.
[6] O. P. BRUNO, E. M. HYDE, AND F. REITICH, *An accelerated solver for penetrable obstacle scattering with tunable order of convergence*, in preparation.
[7] O. P. BRUNO AND A. SEI, *A fast high-order solver for EM scattering from complex penetrable bodies: TE case*, IEEE Trans. Antennas and Propagation, 48 (2000), pp. 1862–1864.

[8] O. P. Bruno and A. Sei, *A fast high-order solver for problems of scattering by heterogeneous bodies*, IEEE Trans. Antennas and Propagation, 51 (2003), pp. 3142–3154.
[9] D. Colton and R. Kress, *Inverse Acoustic and Electromagnetic Scattering Theory*, 2nd ed., Springer-Verlag, Berlin, Heidelberg, New York, 1998.
[10] A. Ditkowski, K. Dridi, and J. S. Hesthaven, *Convergent Cartesian grid methods for Maxwell's equations in complex geometries*, J. Comput. Phys., 170 (2001), pp. 39–80.
[11] G. B. Folland, *Introduction to Partial Differential Equations*, second ed., Princeton University Press, Princeton, NJ, 1995.
[12] D. Gilbarg and N. S. Trudinger, *Elliptic Partial Differential Equations of Second Order*, Springer-Verlag, Berlin, Heidelberg, New York, 1977.
[13] E. Heinz, *Über die Eindeutigkeit beim Cauchyschen Anfangswertproblem einer elliptischen Differentialgleichung zweiter Ordnung*, Nachr. Akad. Wiss. Göttingen. IIa., 1 (1955), pp. 1–12.
[14] E. M. Hyde, *Fast, High-Order Methods for Scattering by Inhomogeneous Media*, Ph.D. thesis, California Institute of Technology, Pasadena, CA, 2003.
[15] E. M. Hyde and O. P. Bruno, *A fast, high-order method for scattering by penetrable bodies in three dimensions*, J. Comput. Phys., 202 (2005), 236–261.
[16] E. M. Hyde and O. P. Bruno, *A fast, high-order method for scattering by inhomogeneous media in three dimensions*, Phys. B, 338 (2003), pp. 82–86.
[17] A. Kirsch and P. Monk, *Convergence analysis of a coupled finite element and spectral method in acoustic scattering*, IMA J. Numer. Anal., 10 (1990), pp. 425–447.
[18] A. Kirsch and P. Monk, *An analysis of the coupling of finite-element and Nyström methods in acoustic scattering*, IMA J. Numer. Anal., 14 (1994), pp. 523–544.
[19] H. Koch and D. Tartaru, *Carleman estimates and unique continuation for second-order elliptic equations with nonsmooth coefficients*, Comm. Pure Appl. Math., 54 (2001), pp. 339–360.
[20] R. Kress, *Linear Integral Equations*, Springer-Verlag, Berlin, 1989.
[21] R. Kress, *Numerical Analysis*, Grad. Texts in Math. 181, Springer-Verlag, New York, 1998.
[22] E. H. Lieb and M. Loss, *Analysis*, Grad. Stud. Math. 14, AMS, Providence, RI, 1997.
[23] G. Liu and S. Gedney, *High-order Nyström solution of the volume EFIE for TM-wave scattering*, Microwave and Optical Technology Letters, 25 (2000), pp. 8–11.
[24] P. A. Martin, *Acoustic scattering by inhomogeneous obstacles*, SIAM J. Appl. Math., 64 (2003), pp. 297–308.
[25] W. H. Press, S. A. Teukolsky, W. T. Vetterling, and B. P. Flannery, *Numerical Recipes in Fortran* 77*: The Art of Scientific Computing*, Vol. 1, 2nd ed., Cambridge University Press, Cambridge, 1992.
[26] W. Rachowicz and L. Demkowicz, *An hp-adaptive finite element method for electromagnetics. Part* 1*: Data structure and constrained approximation*, Comput. Methods Appl. Mech. Engrg., 187 (2000), pp. 307–335.
[27] G. M. Vainikko, *Fast solvers of the Lippmann-Schwinger equation*, in Direct and Inverse Problems of Mathematical Physics (Newark, DE, 1997), R. P. Gilbert, J. Kajiwara, and Y. S. Xu, eds., Int. Soc. Anal. Appl. Comput. 5, Kluwer Acad. Publ., Dordrecht, The Netherlands, 2000, pp. 423–440.
[28] K. F. Warnick and W. C. Chew, *Numerical simulation methods for rough surface scattering*, Waves Random Media, 11 (2001), pp. R1–R30.
[29] J. A. C. Weideman, *Numerical integration of periodic functions: A few examples*, Amer. Math. Monthly, 109 (2002), pp. 21–36.
[30] P. Werner, *Zur mathematischen Theorie akustischer Wellenfelder*, Arch. Ration. Mech. Anal., 6 (1960), pp. 231–260.
[31] X. M. Xu and Q. H. Liu, *Fast spectral-domain method for acoustic scattering problems*, IEEE Trans. Ultrasonics, Ferroelectrics, and Frequency Control, 48 (2001), pp. 522–529.
[32] B. Yang, D. Gottlieb, and J. S. Hesthaven, *Spectral simulations of electromagnetic wave scattering*, J. Comput. Phys., 134 (1997), pp. 216–230.
[33] P. Zwamborn and P. V. den Berg, *Three dimensional weak form of the conjugate gradient FFT method for solving scattering problems*, IEEE Trans. Microwave Theory and Techniques, 40 (1992), pp. 1757–1766.
[34] A. Zygmund, *Trigonometric Series*, 2nd ed., Cambridge University Press, London, 1968.